Available online at www.sciencedirect.com
ScienceDirect
Trans. Nonferrous Met. Soc. China 24(2014) 1446−1451
Transactions of Nonferrous Metals Society of China
www.tnmsc.cn

Preparation and characterization of amorphous boron powder with high activity

Zhi-he DOU, Ting-an ZHANG, Guan-yong SHI, Chao PENG, Ming WEN, Ji-cheng HE

Key Laboratory for Ecological Metallurgy of Multimetallic Mineral (Ministry of Education), Northeastern University, Shenyang 110819, China

Received 20 May 2013; accepted 12 January 2014

Abstract: The amorphous boron powders with high activity were prepared by the high-energy ball milling−combustion synthesis method. The effects of the milling rate and milling time on the crystallinity, microscopic morphology and reactivity of amorphous boron powder were studied. The results show that the crystallinity of amorphous nano-boron powder is only 22.5%, and its purity reaches 92.86%. The high-energy ball milling can significantly refine boron powder particle sizes, whose average particle sizes are smaller than 50 nm, and specific surface areas are of up to 70.03 m^2/g. When the transmission electron beam irradiates the samples, they rapidly melt. It can be seen that the monomer amorphous boron size is less than 30 nm from the specimen melting traces, which indicates that the samples have high reactivity.

Key words: amorphous nano-boron powder; high activity; high-energy ball milling; combustion synthesis

1 Introduction

The traditional metal thermal reduction methods which are used to prepare boron powders have some shortcomings, such as low purity, large particle size and high cost [1−5]. Its purity is only less than 90.0% and the size is larger than 2 μm [6−8]. However, the amorphous nano powder has aroused the great academia interests because of its unique nature. Recently, with the developments of aviation, aerospace, rocket launchers fuel, automotive airbags and nano materials, the demands of amorphous boron powders are increasing [9−11], and especially the demands for the amorphous boron powders with high activity [12]. Now, the qualities of amorphous boron powders have been unable to meet the requirements, so the preparation of the amorphous boron powder with high activity has become the hot topic. The researches mainly concentrate on theoretical calculations of the boron nanotubes and boron nanofibers [13−15]. The preparations and performance characterizations on amorphous boron powders with high reactivity are scarcely.

As for the shortcomings of the large particle size and the low activity of amorphous boron powder prepared by the magnesium thermal reduction, the high-energy ball milling−combustion synthesis method was used to prepare the amorphous nanometer boron powders with high reactivity.

2 Experimental

2.1 Sample preparation

The raw materials included magnesium powder with 99% purity within the particle size less than 149 μm and B_2O_3 powder with 99% purity and particle size less than 149 μm. The materials were weighed stoichiometrically according to the following Equation (1) and then mixed by high-energy ball milling (mode:P4 of Fritsch Company made in Germany). The milling conditions were: balls of 5−15 mm and the volume ratio of reactants to balls of (1−2):1. Before combustion synthesis reactions, the reaction raw materials were mixed, and the details were as follows: for No. A, ordinary tank mixing for 3 h; for No. B, high-energy ball milling for 15 min with 300 r/min; for No. C, high-energy ball milling for 20 min with 300 r/min; for No. D, high-energy ball milling for 20 min with 250 r/min;

Foundation item: Project (51002025) supported by the National Natural Science Foundation of China
Corresponding author: Zhi-he DOU; Tel: +86-13940091053; E-mail: douzh@smm.neu.edu.cn
DOI: 10.1016/S1003-6326(14)63211-8

for No. E, high-energy ball milling for 20 min with 30 r/min. The detailed experiment conditions are listed in Table 1. The mixed powders were placed in a SHS reactor. And the ignitor of $KClO_3$ and magnesium were placed on the surface of reactants to ignite the combustion synthesis reaction to get the coarse products with MgO by-products.

$$3Mg+B_2O_3=2B+3MgO \quad (1)$$

Table 1 Experiment conditions

Sample No.	$n(Mg)/n(B_2O_3)/n(KClO_3)$
A	3.0:1:0
B	3.0:1:0
C	3.0:1:0.1
D	3.0:1:0.1
E	3.0:1:0

The combustion products were leached with 10% HCl in mass fraction at 45 °C for 24 h and amorphous boron powders were obtained after filtration and drying.

2.2 Characterization

The phase compositions of the amorphous boron powder were determined by an X-ray diffractometer (XRD, Rigaku D/max III B) and then the crystallinity was calculated. The microscopic morphology of amorphous boron powder was observed by a scanning electron microscope (SEM, SSX−550 and FEI, NavoSEM). The specific surface area of amorphous boron powder was obtained with a specific surface area and bore diameter tester (ASAP2020M). The amorphous boron powder microscopic morphology was analyzed by a transmission electron microscope (TEM, H800). The reactivity of amorphous boron powders was characterized on their crystallinity and specific surface areas and chemical reaction temperature.

3 Results and discussion

3.1 XRD pattern

Figure 1 shows the XRD patterns of the amorphous boron powders prepared in different conditions. For the sample A, the reactants were mixed by milling for 3 h in ordinary mixing tank. For the samples B−E, the reactants were milled by high-energy ball milling for 15−20 min (the experimental conditions for the samples A−E in Figs. 2−4 and Table 2 were the same as those in Fig. 1, so these were not explained repeatedly).

Figure 1 shows that samples A−D have some obvious diffraction peaks of crystal boron at the 2θ of

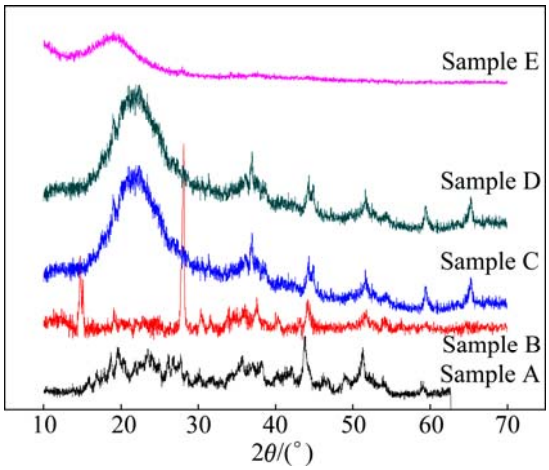

Fig. 1 XRD patterns of boron powders

36.96°, 44.32°, 51.64° and 59.48° which do not appear in sample E. But sample B has a great diffraction peak at 2θ of 28.12° of the crystalline diffraction peak of impurity magnesium borate ($Mg_3B_2O_6$) attributed to the inadequate acid leaching. By comparing the XRD patterns of samples A−D, it is found that the crystal boron diffraction peak intensity in amorphous boron will reduce significantly if the reactants are pretreated through the high-energy ball milling, and the crystallinity of amorphous boron powder declines obviously with the increase in high-energy ball milling time and the high-energy ball milling rate. By comparing XRD patterns of sample C and sample E, it can be seen that the crystallinities of amorphous boron powders will increase with reaction temperature increasing. There is an obvious diffraction peak of crystal boron in the sample C, but there is not in the sample E. Because the heating agent $KClO_3$ was added to the reactants when preparing the sample C, the reaction temperature became high, which provided a completely thermodynamic and kinetic condition for crystal boron to form and grow up. The crystallinities of samples A−E are 72.46%, 32.4%, 31.0%, 29.4% and 22.5%, respectively, which are calculated by software Diffrac.Suite.Eva. By combining XRD and calculated crystallinities, it is found that the samples B−E are mainly amorphous boron. So, the high-energy ball milling for the reactants is necessary to obtain the lower crystallinity amorphous boron powders.

3.2 Morphology

Figure 2 shows the SEM images of the amorphous boron powders made under different conditions. It can be seen from Fig. 2 that boron powder particle sizes are of micron degree and a large number of rod-like crystals appear (the length of about 1 μm, the diameter of

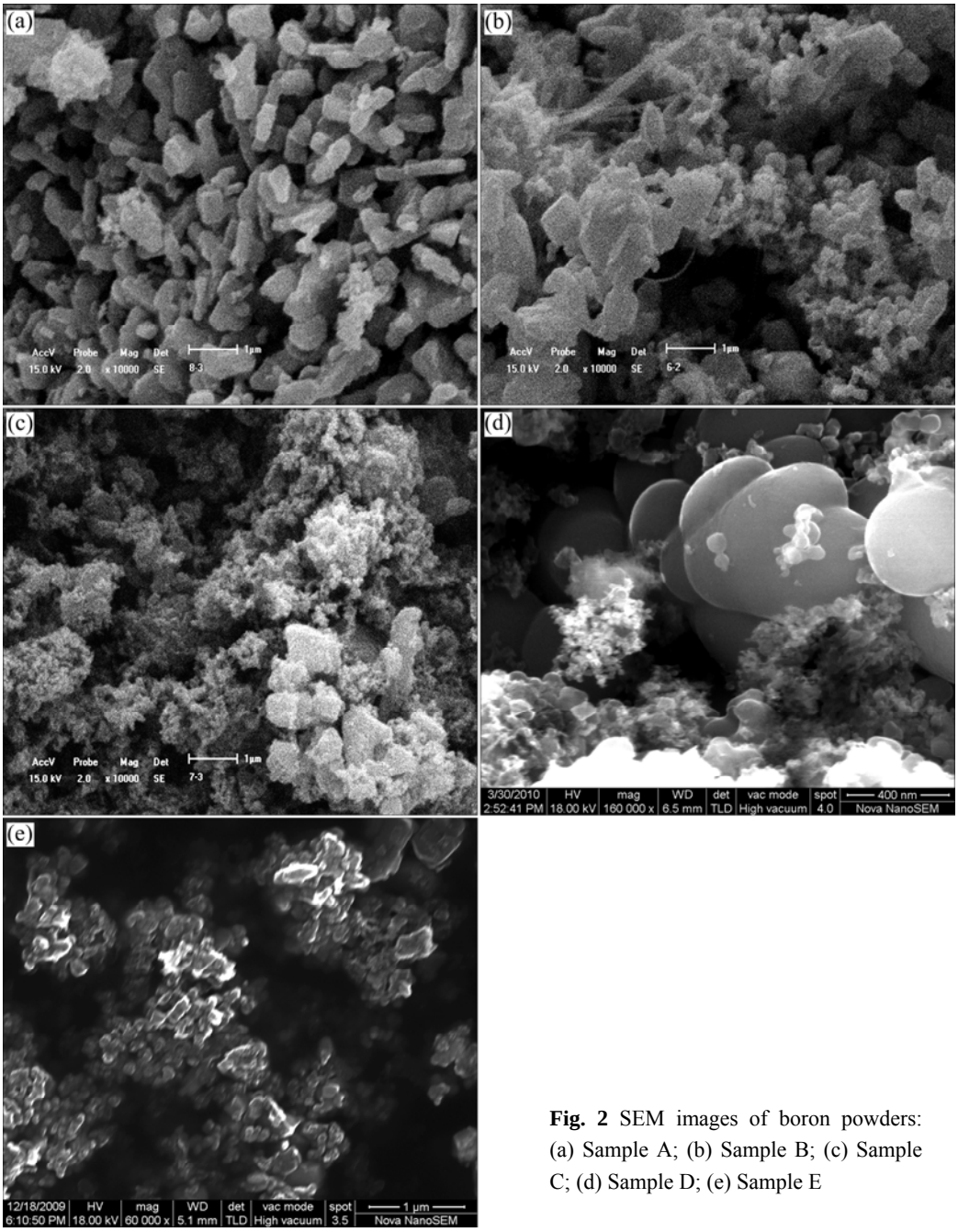

Fig. 2 SEM images of boron powders: (a) Sample A; (b) Sample B; (c) Sample C; (d) Sample D; (e) Sample E

100−200 nm) when the reactants are not milled by high-energy ball milling. The average particle sizes in samples B−E are of nano degree, in which the average particles size of sample B is about 50 nm. But the reunion phenomena appear in the samples B and C. The reunion will result in specific surface areas and reactivity of amorphous boron powders declining. Comparing with the samples B and C, it is found that the particles more than 400 nm appear in sample D (the EDS results show that it is $Mg_3B_2O_6$) and the average particle size of sample E is less than 50 nm. Because the reactant particles are not refined fully when the ball milling rate is low, and at the same time some heating agent $KClO_3$ added to the reactants will increase the reaction temperature, those offer sufficient conditions for crystal particles growth up. The high temperature can make not only the crystal particle grow up better but also the content of crystalline boron in the products increase significantly. With the milling time increasing, the particle size of the boron powders becomes small significantly. Thus, the high-energy ball milling pretreatment is very effective to obtain nanoscale or small boron powders. In order to prepare the amorphous boron powders with high activity, the high-energy ball

milling conditions must be controlled reasonably.

Figure 3 shows the specific surface areas of the amorphous boron powders made in different conditions. It can be seen that the specific surface areas significantly increase with the high-energy ball milling rate and time increasing. The specific surface area of sample A is only 4.22 m^2/g when the reactants are not pretreated by the high-energy ball milling. The specific surface areas of the samples increase significantly after the reactants are pretreated by the high-energy ball milling (the specific surface areas of samples B−E are 53.4, 44.9, 47.42 and 70.03 m^2/g, respectively). Based on the above, it can be concluded that the high-energy ball milling can refine significantly particle sizes to increase the powder specific surface areas, thus improving its reactivity. But the increase of milling rate and milling time will lead to the small boron powder particles gathering together and the apparent surface areas decreasing, which will influence the reactivity. The specific surface areas of the amorphous boron powders decrease significantly with the temperature increasing, which will lead to its chemical reactivity reducing. When preparing the sample C, the heating agent $KClO_3$ is added to the reactants and the reaction temperature is higher.

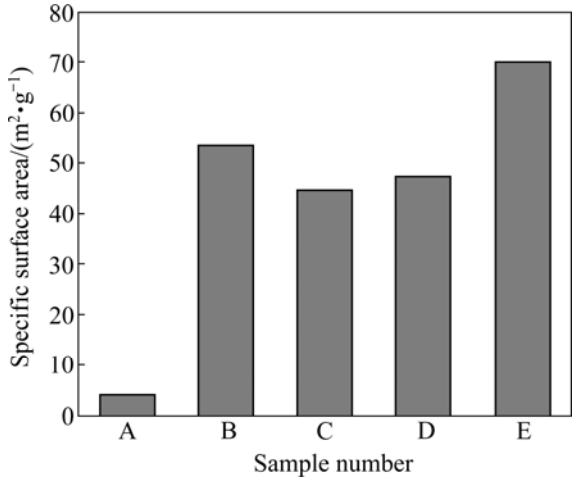

Fig. 3 Specific surface areas of boron powders

During the TEM process, the sample rapidly melts when the transmission electron beam irradiates the sample, which indicates that the sample has a high reactivity. Figure 4 shows that the monomer particle size of amorphous boron powder is less than 30 nm (from the specimen melting traces in Fig. 4), which is consistent with the results of SEM.

3.3 Chemical composition

Table 2 shows the chemical compositions of the amorphous boron prepared in different conditions.

Comparing with sample A, the Mg content in sample C reduces from 13.30% to 7.69% with the ball milling time increasing. Because the high-energy ball can not only enhance the mixed degree among the reactants significantly, but also improve the reactant reactivity to strengthen the reaction degree. Because the collisions occur between the balls and the powders, the captured powders suffer severe plastic deformation during the milling process.

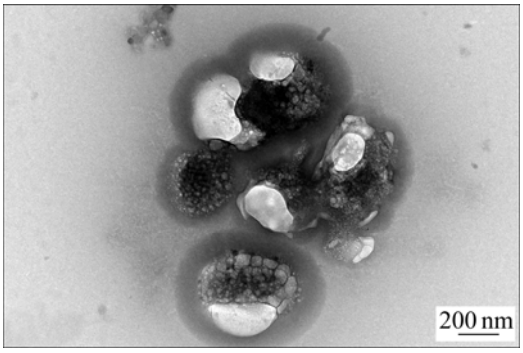

Fig. 4 TEM image of sample E

Table 2 Chemical compositions of boron powders

Sample No.	*w*(B)/%	*w*(Mg)/%	*w*(Fe)/%
A	85.03	13.30	0.07
B	88.71	9.86	0.05
C	90.76	7.69	0.05
D	92.07	6.89	0.04
E	92.86	6.47	0.03

High-density defects and nano interface produced during the ball milling process promote greatly the SHS reaction and they play a leading role. A lot of magnesium would vaporize and volatile during the combustion synthesis reaction process, which led to Mg local deficiency(locally excessive B_2O_3). The generated MgO reacted with the locally excessive B_2O_3 to generate $Mg_3B_2O_6$ by-product, resulting in the boron purity declining. The high-energy ball milling can refine reactant particle by the collision and forging among the pellets, they reach the effects of combination and "welding" at a atomic level, which increases the reactant activities. Once the reaction occurs, it will finish quickly, just a moment to avoid the reactants excessive locally or insufficient during the reaction process. The impurity Mg content reduces significantly when the ball milling rate increases.

3.4 Amorphous boron activity

In this work, the chemical activities of the amorphous boron powders were qualitatively

characterized through the crystallinities of the amorphous boron powders and reaction temperature of synthesizing boride as a raw materials.

In order to study the chemical reactivity of amorphous boron powder, a special research was made on the activity differences between sample E and the commercial nano amorphous boron powder (its XRD is shown in Fig. 5) in Ref. [14]. During the process of synthesizing LaB_6 using sample E and commercial boron powder as materials, the reaction temperature of sample E is lower 150 °C than commercial boron (shown in Fig. 6). The particle size of LaB_6 synthesized using the sample E as material is only 150 nm, while it is more than 2 μm using commercial boron powder as materials, which limits the LaB_6 electrical performance severely (shown in Fig. 7).

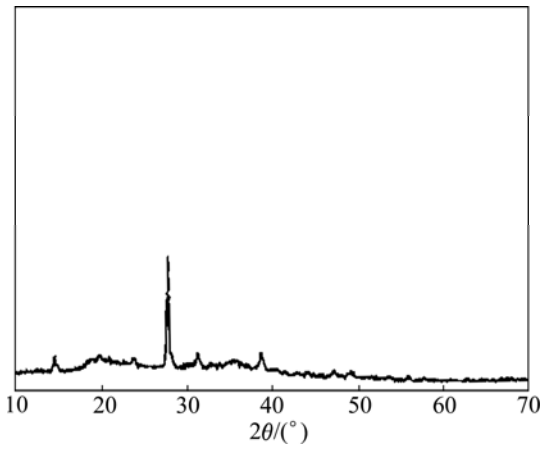

Fig. 5 XRD pattern of commercial boron powders

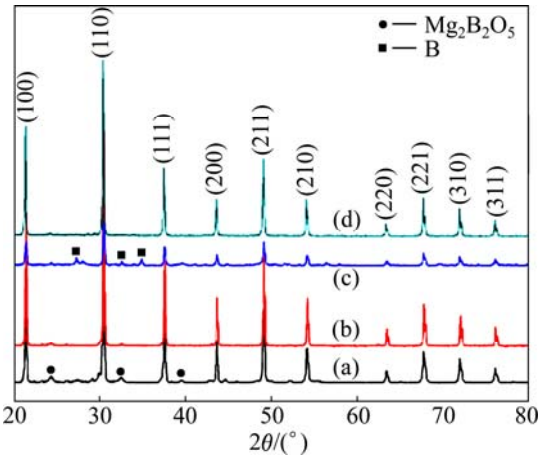

Fig. 6 XRD patterns of bulk LaB_6 from amorphous B+La powders sintered at 1200 °C (a) and 1400 °C (b), commercial B+La powders sintered at 1250 °C (c) and 1350 °C (d)

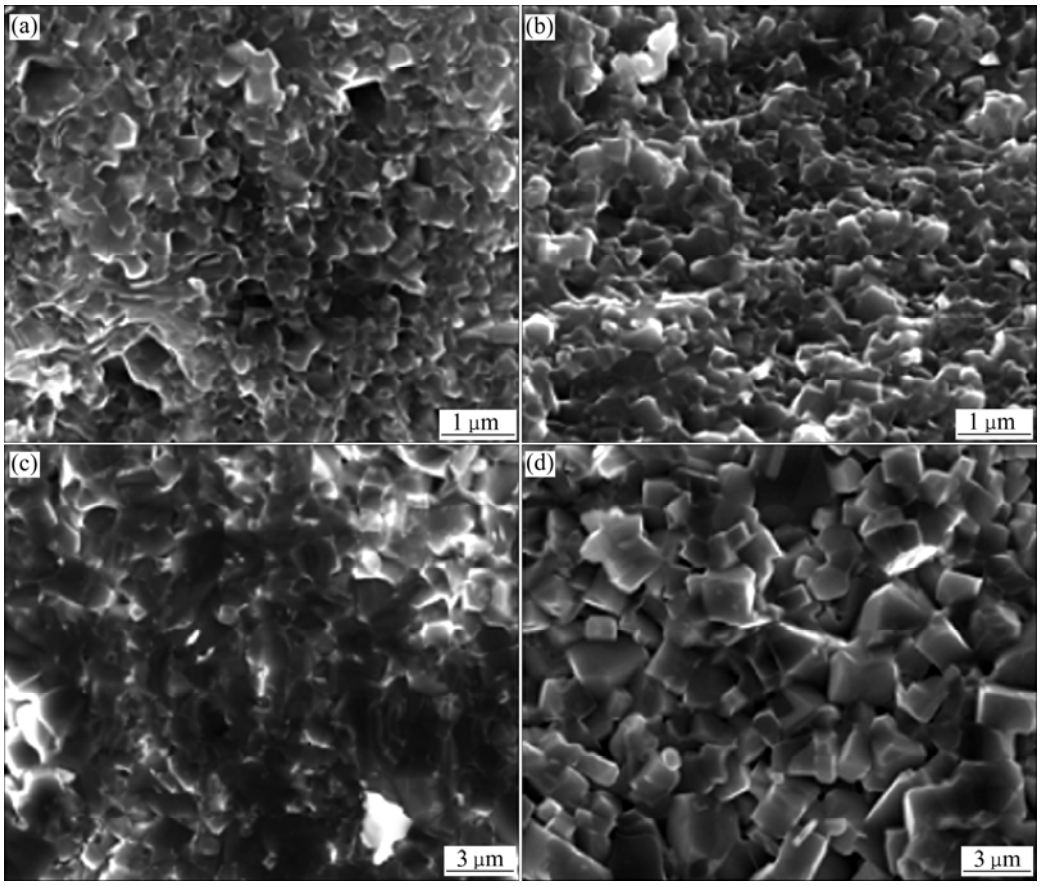

Fig. 7 SEM images of fracture surface of bulks LaB_6 from amorphous B+La powders sintered at 1200 °C (a) and 1350 °C (b), commercial B+La powders sintered at 1250 °C (c) and 1350 °C (d)

4 Conclusions

1) The amorphous nanometer boron powders with high activity were prepared by the high-energy ball milling−combustion synthesis method. Their crystallinity is only 22.5%, and their purity reaches 92.86%.

2) The high-energy ball milling can significantly refine boron powder particle sizes, whose average particle sizes are smaller than 50 nm, the specific surface areas are 70.03 m^2/g. The sample has a high reaction interface and reactivity.

3) During the TEM analysis process, the sample rapidly melts when the transmission electron beam irradiates the sample, which indicates that the sample has a high reactivity. The specimen melting traces show that the monomer particle size of amorphous boron powder is less than 30 nm, but the apparent reunion phenomena appear.

References

[1] SIBERCHIOT B, CLEROUIN J. An equation of state of amorphous β-boron under high pressure [J]. Solid−Solid Phase Transformations in Inorganic Materials, 2011, 172−174: 1220−1221.

[2] TILEKAR K V, GAJBHIVE V P, PRASANTH H, SOMAN T. Preparation of high purity amorphous boron powder [J]. Defence Science Journal, 2005, 55(4): 471−475.

[3] WU Ji-jun, ZHAI Yu-chun, ZHANG Guang-li, YANG Bin, DAI Yong-nian. Preparation of amorphous boron powder by magnesiothermic reduction of B_2O_3 and micro-structural analysis of products [J]. Journal of Northeastern University: Natural Science, 2009, 30(S2): 216−219. (in Chinese)

[4] PANG Wei-qiang, ZHANG Jiao-qiang, ZHANG Qiong-fang, HU Song-qi, GUO Ji-ying. Coating of boron particles and combustion residue analysis of boron-based solid propellants [J]. Journal of Solid Rocket Technology, 2006, 29(3): 204−207. (in Chinese)

[5] WANG P, ORIMO S, FUJII H. Characterization of hydrogenated amorphous boron by a combination of infrared absorption spectroscopy and thermal analyses [J]. Journal of Alloys and Compounds, 2003, 359(1−2): L1−L3.

[6] TAREQ A H, JACOB K, MICHAEL E. The use of boron for thermochemical storage and distribution of solar energy [J]. Solar Energy, 2007, 81(1): 93−101.

[7] WANG P, ORIMO S, TANABE K, FUJII H. Hydrogen in mechanically milled amorphous boron [J]. Journal of Alloys and Compounds, 2003, 350(1−2): 218−221.

[8] DOU Zhi-he, ZHANG Ting-an, WANG Yan-li. Primary research on preparation of boron powder by self-propagating high-temperature synthesis with a stage of metallurgy [J]. Journal of Northeastern University: Natural Science, 2005, 26(1): 63−66. (in Chinese)

[9] WU Ji-jun, ZHAI Yu-chun, ZHANG Guang-li, LIU Da-chun, XIE Ke-qiang, DAI Yong-nian. Leaching of combustion products in preparing amorphous boron powder by magnesiothermic reduction [J]. Journal of Northeastern University: Natural Science, 2009, 30(S2): 6−10. (in Chinese)

[10] SONG Ming-zhi, AN Hui, ZHAO Jun. Preparation of boron by molten-salt electrolysis [J]. Liaoning Chemical Industry, 2004, 33(8): 469−470. (in Chinese)

[11] WANG Y Q, DUAN X F, CAO L M, LI G, WANG W K. Application of energy-filtering transmission electron microscopy to characterize amorphous boron nanowires [J]. Journal of Crystal Growth, 2002, 244: 123−128.

[12] SHALAMBERIDZE S O, KALANDADZE G I, KHULELIDZE D E, TSURTSUMIA B D. Production of α-rhombohedral boron by amorphous boron crystallization [J]. Journal of Solid State Chemistry, 2000, 154(1): 199−203.

[13] BAO Li-hong, ZHANG Jiu-xing, ZHOU Shen-lin, WEI Yong-feng, DOU Zhi-he. The effect of precursor boron nanopowder on the microstructure and emission properties of LaB_6 cathode materials [J]. Physica Status Solidi (c) Current Topics in Solid State Physics, 2012, 9(1): 11−14.

[14] ZHU D M, KISI E. Synthesis and characterization of boron/boron oxide nanorods [J]. Journal of the Australian Ceramic Society, 2009, 45(2): 49−53.

[15] NOGI N, NODA T, TANAKA S. Phonen properties of isotopically modified β rhombohedral boron [J]. Journal of Solid State Chem, 2000, 154: 296−300.

高活性无定形硼粉的制备及表征

豆志河，张廷安，史冠勇，彭 超，文 明，赫冀成

东北大学 多金属共生矿生态化冶金教育部重点实验室，沈阳 110819

摘 要：采用高能球磨−燃烧合成法制备高活性无定形纳米硼粉。考察球磨转速、球磨时间等因素对无定形硼粉结晶度、微观形貌以及反应活性等性能的影响。结果表明：无定形纳米硼粉结晶度只有 22.5%，纯度达 92.86%；高能球磨预处理显著细化了硼粉粒径，平均粒径在 50 nm 以下，比表面积达 70.03 m^2/g。当透射电子束照射到试样时，试样快速熔化。由试样熔化痕迹可看出无定形硼粉单体颗粒粒径小于 30 nm，说明试样具有极高的反应活性。

关键词：无定形纳米硼粉；高活性；高能球磨；燃烧合成

(Edited by Hua YANG)